

LETTER

Computationally Efficient Reflectance Estimation for Hyperspectral Images*

Takaaki OKABE^{†a)}, *Nonmember* and Masahiro OKUDA[†], *Member*

SUMMARY The Retinex theory assumes that large intensity changes correspond to reflectance edges, while smoothly-varying regions are due to shading. Some algorithms based on the theory adopt simple thresholding schemes and achieve adequate results for reflectance estimation. In this paper, we present a practical reflectance estimation technique for hyperspectral images. Our method is realized simply by thresholding singular values of a matrix calculated from scaled pixel values. In the method, we estimate the reflectance image by measuring spectral similarity between two adjacent pixels. We demonstrate that our thresholding scheme effectively estimates the reflectance and outperforms the Retinex-based thresholding. In particular, our methods can precisely distinguish edges caused by reflectance change and shadows.

key words: *hyperspectral image, retinex, reflectance estimation, singular values*

1. Introduction

Recent advances in hyperspectral imaging allow us to acquire rich spectral information. Unlike the traditional RGB sensing, hyperspectral images can provide almost continuous spectral information. The remote sensing technology based on the hyperspectral imaging is now a powerful observation technique for investigating ground materials. In addition, the use of the spectral information improves capability in image processing techniques like classification and target detection and realizes many practical applications such as environmental monitoring and food analysis [1]–[6]. In the applications, the reflectance information is more preferable than radiance acquired by image sensors, since colored illumination and shadows often degrade the performance of image processing, and thus it is important to develop reflectance estimation algorithms.

In the image processing literature, many methods for the reflectance estimation have been proposed [7]–[21]. Barrow and Tenenbaum [13] introduced a method of intrinsic image decomposition, which separates reflectance and shading components. The reflectance component involves a specific object color that does not depend on scene illumination, while the shading component mainly depends on illumination and surface geometry. The intrinsic image decomposition is a major challenge due to its ill-posedness, in

which there are two unknown components for one observed image, and hence many of conventional methods need time consuming steps. This can be a significant drawback for handling large data like the hyperspectral images. The well-known Retinex algorithm originally proposed in [22] assumes that large intensity changes correspond to reflectance edges, while smoothly-varying regions are due to shading. This traditional algorithm merely performs simple thresholding, but it still works well both for grayscale and color images [15].

In this paper, we introduce a simple and practical method for reflectance estimation of hyperspectral images. We show that the spectral information provides us with the necessary information to determine the gradients of a reflectance image. Our method is realized simply by thresholding singular values of a matrix calculated from scaled pixels values. This allows us to employ effective thresholding with low computational complexity. One of challenging tasks in the reflectance estimation is to distinguish edges caused by the reflectance change and shadows. Experimental results show that our method can precisely distinguish the two types of edges and outperforms the Retinex-based thresholding.

Notation: For a hyperspectral image \mathbf{I} , let the number of spectral bands and the number of pixels in a band be M and N , respectively. We denote the m -th spectral plain by $\mathbf{I}_m \in \mathbb{R}^N$ ($m = 1, 2, \dots, M$), and its pixel value at a position (x, y) by $\mathbf{I}_{(x,y,m)} \in \mathbb{R}$. Let \mathbf{D}_x and \mathbf{D}_y be differential operators w.r.t horizontal and vertical directions, respectively. For any 2D matrix \mathbf{X} , we denote the (x, y) -th element of \mathbf{X} by $[\mathbf{X}]_{(x,y)} \in \mathbb{R}$.

2. Reflectance Estimation by Gradient Thresholding

2.1 Lambertian Model

Colors captured by a sensor complicatedly depend on light with various environments such as illumination, scene geometry, and materials. One of the simplest models for radiance description is the Lambertian reflectance model. Under the Lambertian circumstances, the radiance towards an observer at a non-emissive point is expressed by

$$\hat{\mathbf{I}} = \int r(\lambda)l(\lambda)d\lambda \cdot \cos \theta,$$

where $r(\lambda)$ is a surface reflectance (albedo), $l(\lambda)$ is an illumination, and λ is the wavelength. It also depends on the

Manuscript received March 6, 2017.

Manuscript revised May 10, 2017.

Manuscript publicized May 26, 2017.

[†]The authors are with the Faculty of Environmental Engineering, The University of Kitakyushu, Kitakyushu-shi, 808–0135 Japan.

*This work is supported by MICSCOPE Project.

a) E-mail: x6mca006@eng.kitakyu-u.ac.jp

DOI: 10.1587/transinf.2017EDL8051

angle θ between the direction of an incident light and a surface normal. Under the white illumination with a uniform spectral distribution, it is rewritten as

$$\hat{\mathbf{I}} = \int r(\lambda)d\lambda \cdot K \cos \theta.$$

Now, the illuminance at a pixel (x, y) captured by a sensor with the spectral sensitivity $c(\lambda)$ is modeled as

$$\hat{\mathbf{I}}_{(x,y)} = \int r(\lambda)l(\lambda)c(\lambda)d\lambda \cdot \cos \theta.$$

Assume that the camera sensor has a piecewise flat spectral sensitivity in the range of the wavelengths $[\lambda_m, \lambda_{m+1}]$, and the illumination is also flat in the range, then the captured illuminance in the m -th band $\hat{\mathbf{I}}_{(x,y,m)}$ is given by

$$\hat{\mathbf{I}}_{(x,y,m)} = \int_{\lambda_m}^{\lambda_{m+1}} r(\lambda)d\lambda \cdot K'_m \cos \theta,$$

where K'_m is a constant value determined by the sensitivity function and the illumination. Letting the reflectance and the shading component be $\hat{\mathbf{R}}_{(x,y,m)} = \int_{\lambda_m}^{\lambda_{m+1}} r(\lambda)d\lambda$ and $\hat{\mathbf{S}}_{(x,y,m)} = K'_m \cos \theta$, respectively, $\hat{\mathbf{I}}_{(x,y,m)}$ is given by the product of the two components,

$$\hat{\mathbf{I}}_{(x,y,m)} = \hat{\mathbf{R}}_{(x,y,m)} \cdot \hat{\mathbf{S}}_{(x,y,m)}.$$

By taking the logarithm of the images, $\mathbf{R}_{(x,y,m)} = \log \hat{\mathbf{R}}_{(x,y,m)}$ and $\mathbf{S}_{(x,y,m)} = \log \hat{\mathbf{S}}_{(x,y,m)}$, the observed image is expressed by the sum of the two images in the log domain as

$$\mathbf{I}_{(x,y,m)} = \mathbf{R}_{(x,y,m)} + \mathbf{S}_{(x,y,m)}. \quad (1)$$

2.2 Conventional Retinex-Based Thresholding

Our goal is to estimate the reflectance component \mathbf{R} from the observed image \mathbf{I} . This estimation is inherently a challenging problem since the Eq. (1) is severely underdetermined. One solution is to apply tractable prior knowledge to solve the problem [11], [14], [15]. The well-known Retinex algorithm [22], which many conventional methods are built upon, is based on a simple assumption that a reflectance image has piecewise constant regions with sharp edges, whereas the shading image smoothly varies between pixels. Based on the Retinex principle, sharp intensity changes should be retained, while the small changes are factored out. This is fulfilled simply by thresholding the gradients of the observed log image

$$[\mathbf{D}_h \mathbf{R}_m]_{(x,y)} = \begin{cases} [\mathbf{D}_h \mathbf{I}_m]_{(x,y)} & \text{if } |[\mathbf{D}_h \mathbf{I}_m]_{(x,y)}| > T_r \\ 0 & \text{otherwise} \end{cases}, \quad (2)$$

where $\mathbf{D}_h \in \mathbb{R}^N$ represents the difference operator along the horizontal direction, and T_r is a threshold. The same procedure is employed for the vertical direction.

3. Singular Value Thresholding

Varying illumination caused by light sources, shapes of objects, and terrains alters the amplitudes of spectra. Figure 1 shows the spectra of the two pixels in the same material. The pixels are located in the regions separated by the edge caused by the shadows, and thus the shape of the spectra is similar, but they vary in intensity. To exploit the spectral variation, we first find the scaling parameter $n_h^{(x,y)}$, which minimizes the mean squared error between the adjacent pixels

$$\min_{n_h^{(x,y)}} \sum_{m=1}^M (\hat{\mathbf{I}}_{(x,y,m)} - n_h^{(x,y)} \hat{\mathbf{I}}_{(x+1,y,m)})^2,$$

where M is the number of bands. The solution of the problem is given by

$$n_h^{(x,y)} = \frac{\sum_{m=1}^M \hat{\mathbf{I}}_{(x,y,m)} \cdot \hat{\mathbf{I}}_{(x+1,y,m)}}{\sum_{m=1}^M \hat{\mathbf{I}}_{(x+1,y,m)}^2}.$$

Next, we find the singular values of the matrix $[\mathbf{A}_h^{(x,y)}]^T \mathbf{A}_h^{(x,y)}$, where $\mathbf{A}_h^{(x,y)}$ is given by

$$\mathbf{A}_h^{(x,y)} = \begin{bmatrix} \hat{\mathbf{I}}_{(x,y,1)} & n_h^{(x,y)} \cdot \hat{\mathbf{I}}_{(x+1,y,1)} \\ \hat{\mathbf{I}}_{(x,y,2)} & n_h^{(x,y)} \cdot \hat{\mathbf{I}}_{(x+1,y,2)} \\ \vdots & \vdots \\ \hat{\mathbf{I}}_{(x,y,M)} & n_h^{(x,y)} \cdot \hat{\mathbf{I}}_{(x+1,y,M)} \end{bmatrix}.$$

The matrix $\mathbf{A}_h^{(x,y)}$ consists of the spectral values of horizontally adjacent pixels at positions (x, y) and $(x+1, y)$, and then $[\mathbf{A}_h^{(x,y)}]^T \mathbf{A}_h^{(x,y)}$ calculates the correlation w.r.t. the spectral information. The size of $[\mathbf{A}_h^{(x,y)}]^T \mathbf{A}_h^{(x,y)}$ is 2×2 , and its singular values are denoted by $\sqrt{\lambda_-}$ and $\sqrt{\lambda_+}$ ($\sqrt{\lambda_-} \leq \sqrt{\lambda_+}$). Our method assumes that the reflectances on two adjacent pixels are similar, the spectra of the two pixels are similar in shape, even if those intensities are different (Fig. 1). When the spectra of the two pixels are similar in shape (i.e. the difference of the two is close to constant), the smallest singular value, $\sqrt{\lambda_-}$, becomes small. In the ideal situation, one can

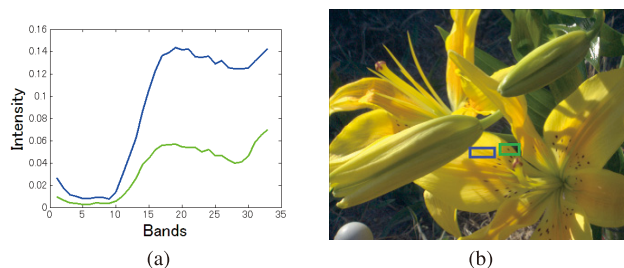


Fig. 1 (a) Spectra of two pixels separated by the edge caused by shadows in (b).

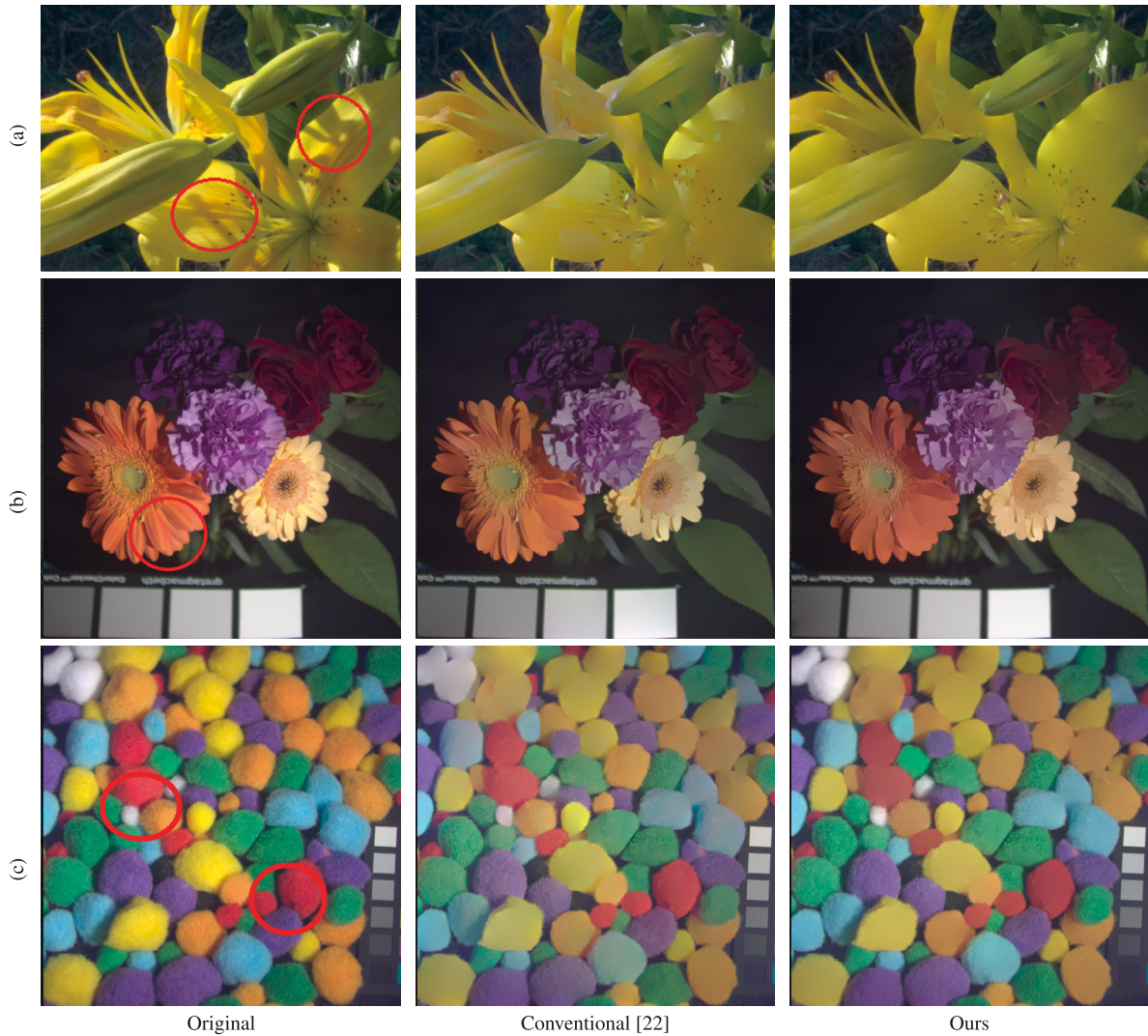


Fig. 2 Comparison with the conventional method [22].

distinguish edges of reflectance images from ones caused by shadows by thresholding $\sqrt{\lambda_-}$. Thus our method allocate the edge at (x, y) to the reflectance edge if the ratio of the smallest singular value is larger than a threshold T_s , which is denoted as

$$[\mathbf{D}_h \mathbf{R}_m]_{(x,y)} = \begin{cases} [\mathbf{D}_h \mathbf{I}_m]_{(x,y)} & \text{if } \frac{\sqrt{\lambda_-}}{\|\mathbf{A}_h^{(x,y)}\|_*} > T_s \\ 0 & \text{otherwise} \end{cases}, \quad (3)$$

where $\|\cdot\|_*$ is the nuclear norm. The nuclear norm is defined as the sum of the singular values of a matrix. In (3), the smallest singular value is divided by the nuclear norm in order to make the values independent to the intensities of the pixels representing $\mathbf{A}_h^{(x,y)}$. The same procedure is employed in the vertical direction.

4. Numerical Results

We compare our method with the Retinex-based threshold-

Table 1 Data set description used in the experiment.

Data Set	Size ($h \times w \times M(\text{bands})$)	Spectral Resolution
(a) [23]	$234 \times 316 \times 33$	400 – 720nm (10nm)
(b) [24]	$512 \times 512 \times 31$	400 – 700nm (10nm)
(c) [24]	$512 \times 512 \times 31$	400 – 700nm (10nm)

ing in Sect. 2.2. Although there are many non-heuristic methods on the reflectance estimation, many of them involves time consuming iterative steps or optimization. On the other hand, the Retinex-based thresholding has much less computational complexity, and it still has higher performances than other computationally efficient methods [15]. In both of our method and the Retinex, final results are reconstructed from the gradient domain by solving the Poisson equation. Table 1 describes the detail of the tested sample images.

Figure 2 and Table 2 show the resultant images and execution time. We manually adjusted the threshold and adopted the largest threshold that preserves the sharp edges

Table 2 Execution time.

Data Set	Retinex	Ours
(a)	0.1142 [s]	0.3615 [s]
(b)	0.3009 [s]	1.1074 [s]
(c)	0.2952 [s]	1.1089 [s]

of the reflectance in both of our and the conventional method. The sharp edges due to the illumination remain in the results of the Retinex, while our results relieve the influence of the sharp shadows and more precisely estimate the reflectance and distinguish edges caused by the reflectance change and shadows, especially for the regions circled by red in Fig. 2.

5. Conclusions

We proposed the technique for the reflectance estimation based on simple thresholding. Comparing with the conventional Retinex, which allocate the edges to the reflectance and shading based on the intensity of the edges, our method achieves more convincing estimation.

References

- [1] Y.-Q. Zhao and J. Yang, "Hyperspectral image denoising via sparse representation and low-rank constraint," *The Imaging Science Journal*, vol.53, no.1, pp.296–308, 2015.
- [2] P.W. Yuen and M. Richardson, "An introduction to hyperspectral imaging and its application for security, surveillance and target acquisition," *IEEE Trans. Geosci. Remote Sens.*, vol.58, no.5, pp.241–253, May 2010.
- [3] C. Chang, *Hyperspectral Data Processing: Algorithm Design and Analysis*, Wiley, 2013.
- [4] J.M. Bioucas-Dias, A. Plaza, G. Camps-Valls, P. Scheunders, N. Nasrabadi, and J. Chanussot, "Hyperspectral remote sensing data analysis and future challenges," *Geoscience and Remote Sensing Magazine*, IEEE, vol.1, no.2, pp.6–36, 2013.
- [5] M. Rizkinia, T. Baba, K. Shirai, and M. Okuda, "Local spectral component decomposition for multi-channel image denoising," *IEEE Transactions on Image Processing*, vol.25, no.7, pp.3208–3218, 2016.
- [6] M. Rizkinia and M. Okuda, "Local abundance regularization for hyperspectral sparse unmixing," *Signal and Information Processing Association Annual Summit and Conference (APSIPA)*, 2016 Asia-Pacific, pp.1–6, IEEE, 2016.
- [7] E. Hsu, T. Mertens, S. Paris, S. Avidan, and F. Durand, "Light mixture estimation for spatially varying white balance," *ACM Trans. Graph.*, vol.27, no.3, pp.70:1–70:7, 2008.
- [8] B.V. Funt, M.S. Drew, and M. Brockington, "Recovering shading from color images," *ECCV-92: Second European Conference on Computer Vision*, pp.124–132, Springer-Verlag, 1992.
- [9] A. Bousseau, S. Paris, and F. Durand, "User-assisted intrinsic images," *ACM Trans. Graph.*, vol.28, no.5, pp.130:1–130:10, 2009.
- [10] A. Levin and Y. Weiss, "User assisted separation of reflections from a single image using a sparsity prior," *ECCV (1)*, ed. T. Pajdla and J. Matas, vol.3021, pp.602–613, Springer, 2004.
- [11] Y. Li and M.S. Brown, "Single image layer separation using relative smoothness," *Proceedings of the 2014 IEEE Conference on Computer Vision and Pattern Recognition, CVPR '14*, pp.2752–2759, IEEE Computer Society, 2014.
- [12] A. Gijsenij and T. Gevers, "Color constancy using natural image statistics," *IEEE Conference on Computer Vision and Pattern Recognition*, IEEE Computer Society, 2007.
- [13] H.G. Barrow and J.M. Tenenbaum, "Recovering intrinsic scene characteristics from images," *Tech. Rep. 157*, AI Center, SRI International, April 1978.
- [14] M.F. Tappen, W.T. Freeman, and E.H. Adelson, "Recovering intrinsic images from a single image," *IEEE Transactions on Pattern Analysis and Machine Intelligence*, vol.27, no.9, pp.1459–1472, 2005.
- [15] R. Grosse, M.K. Johnson, E.H. Adelson, and W.T. Freeman, "Ground-truth dataset and baseline evaluations for intrinsic image algorithms," *International Conference on Computer Vision*, pp.2335–2342, 2009.
- [16] P.-Y. Laffont, A. Bousseau, S. Paris, F. Durand, and G. Drettakis, "Coherent intrinsic images from photo collections," *ACM Trans. Graph.*, vol.31, no.6, pp.202:1–202:11, Nov. 2012.
- [17] E. Garces, A. Munoz, J. Lopez-Moreno, and D. Gutierrez, "Intrinsic images by clustering," *Comp. Graph. Forum*, vol.31, no.4, pp.1415–1424, June 2012.
- [18] Q. Chen and V. Koltun, "A simple model for intrinsic image decomposition with depth cues," *Proceedings of the 2013 IEEE International Conference on Computer Vision, ICCV '13*, pp.241–248, IEEE Computer Society, 2013.
- [19] Q. Zhao, P. Tan, Q. Dai, L. Shen, E. Wu, and S. Lin, "A closed-form solution to retinex with nonlocal texture constraints," *IEEE Trans. Pattern Anal. Mach. Intell.*, vol.34, no.7, pp.1437–1444, 2012.
- [20] Y. Weiss, "Deriving intrinsic images from image sequences," *International Conference on Computer Vision*, pp.68–75, 2001.
- [21] R. Matsuoka, T. Baba, M. Rizkinia, and M. Okuda, "White balancing by using multiple images via intrinsic image decomposition," *IEICE Transactions on Information and Systems*, vol.E98-D, no.8, pp.1562–1570, 2015.
- [22] E.H. Land and J.J. McCann, "Lightness and retinex theory," *JOSA*, vol.61, no.1, pp.1–11, 1971.
- [23] D.H. Foster, K. Amano, S.M.C. Nascimento, and M.J. Foster, "Frequency of metamerism in natural scenes," *Journal of the Optical Society of America A*, vol.23, no.10, pp.2359–2372, 2006.
- [24] T.C.L. at Columbia University Databases.
<http://www.cs.columbia.edu/CAVE/databases/>